Anal Bioanal Chem (2012) 402:2817–2826
DOI 10.1007/s00216-012-5733-0

ORIGINAL PAPER

A label-free electrochemical DNA biosensor based on a Zr(IV)-coordinated DNA duplex immobilised on a carbon nanofibre|chitosan layer

Patoommarn Wipawakarn · Huangxian Ju · Danny K. Y. Wong

Received: 21 November 2011 / Revised: 20 December 2011 / Accepted: 9 January 2012 / Published online: 2 February 2012

Abstract A label-free electrochemical biosensor for detecting DNA hybridisation was developed by monitoring the change in the voltammetric activity of ferrocenecarboxylic acid at the biosensor–solution interface. The biosensor was constructed by initially immobilising on a glassy carbon electrode an anchoring layer consisting of chitosan, carboxyl group functionalised carbon nanofibres and glutaraldehye. Chitosan acted as an adhering agent and carbon nanofibres were strategically used to provide a large surface area with binding points for DNA immobilisation, while glutaraldehye was a linker for DNA probes on the electrode surface. Based on a two-factorial design, cyclic voltammetry of $[Fe(CN)_6]^{3-/4-}$ was performed to optimise the composition of the anchoring layer. Next, a 17-base pair DNA probe was attached to the anchoring layer, followed by its complementary target. Zr(IV) ion, known to exhibit affinity for oxygen-containing electroactive markers, for example, ferrocenecarboxylic acid, was then coordinated in the DNA duplex. In this way, ferrocenecarboxylic acid was attracted towards the biosensor for oxidation. A change in the voltammetric oxidation current of ferrocenecarboxylic acid pre- and post-hybridisation was used to provide an indication of hybridisation. A linear dynamic range between 0.5 and 40 nM and a detection limit of 88 pM of DNA target were then achieved. In addition, the biosensor exhibited good selectivity, repeatability and stability for the determination of DNA sequences.

P. Wipawakarn · D. K. Y. Wong (✉)
Department of Chemistry and Biomolecular Sciences,
Macquarie University,
Sydney, NSW 2109, Australia
e-mail: danny.wong@mq.edu.au

H. Ju
Key Laboratory of Analytical Chemistry for Life Science
(Ministry of Education of China), Department of Chemistry,
Nanjing University,
Nanjing 210093, China

Keywords Electrochemical DNA sensor · Label-free detection · Zr(IV)-coordinated DNA duplex · Carbon nanofibre · Chitosan

Introduction

Hybridisation between a DNA probe and its complementary target plays a pivotal role in the success of drug discovery [1, 2], pathogen detection [3, 4], forensic identifications [5, 6], etc. Several analytical techniques, for example, fluorescence [7], electrochemiluminescence [8], quartz crystal microbalance [9], atomic force microscopy [10] and surface plasma resonance [11], have been developed to detect DNA hybridisation. However, electrochemical methods often offer advantages including simplicity, low cost, sensitivity, fast response time and minimal power requirements over other techniques [12–14]. In developing an electrochemical DNA biosensor, a single-stranded DNA (ssDNA) probe is initially immobilised on an electrode surface, which is then allowed to hybridise with its complementary target sequence. Changes in the resulting interfacial electrode-solution properties such as charge [15], capacitance [16], resistance [17], mass or thickness [18, 19], are subsequently used as evidence for hybridisation.

One of the recent strategies for developing DNA biosensors involves the application of nanomaterials, for example, gold nanoparticles [20], silver nanoparticles [21] and quantum dots [22]. There has also been an increasing interest in the use of other nanomaterials, carbon nanotubes and carbon nanofibres, due to their unique properties in structure, high biocompatibility, high chemical stability, high surface area, high mechanical properties and chemical properties [23, 24]. Although carbon nanotubes have been reported to improve DNA detection by increasing the electroactive surface area by 20% to 40% for probe immobilisation [25], insolubility

of carbon nanotubes in many solvents is a main drawback for their widespread use. In contrast to carbon nanotubes, oxidised carbon nanofibres consist of oxygen-containing groups that aid in resisting their backbone structures from degradation, giving rise to improved wettability [26]. Further, carbon nanofibres are cylindrical nanostructures with graphene layers arranged as stacked cones, cups or plates to yield lengths of micrometer order, while their diameter varies between some tens of nanometers to several hundred nanometers [27]. Carbon nanofibres are also easily mass-produced at a lower cost, better mechanical stability, and a larger surface-active groups-to-volume ratio than carbon nanotubes [28]. Owing to their physical and chemical properties, carbon nanofibres possess a lot of edge sites on the outer wall, leading to high tensile strength, elastic modulus, high thermal and electric conductivity, which facilitate electron-transfer reactions of analytes [29]. For example, carbon nanofibre-coated electrodes exhibited excellent catalytic activity towards the reduction of hydrogen peroxide, making them suitable for use in the rapid flow injection amperometric detection of hydrogen peroxide [30]. Similarly, controlled potentiometry at a soluble carbon nanofibre-doped chitosan film provided a biocompatible and conductive interface for immobilisation and electrochemical detection of leukaemia K562 cells [31].

Very often, the activity of an electroactive label is used to indicate hybridisation at electrochemical DNA biosensors. In this method, a DNA target is initially conjugated with an electroactive label. Hybridisation between a complementary DNA probe already immobilised on an electrode surface and the DNA target would position the electroactive label close to the electrode surface. Application of a suitable potential will then promote a facile electron-transfer reaction of the label at the electrode [32]. Hence, methods involving an electroactive label often exhibit a very low detection limit. For example, Gao et al. [21] reported a detection limit as low as 10 fM in detecting DNA hybridisation based on a probe labelled with multiwalled carbon nanotubes loaded with silver nanoparticles, while Liao et al. [33] estimated a detection limit of 100 pM using a probe labelled with a ferrocenyl peptide. However, in these methods, a substantially long duration and complex steps for attaching the electroactive species to the target DNA are needed before hybridisation. These had prompted the development of simpler label-free methods that offer an immediate detection of hybridisation. In label-free methods, the change in activity of an electroactive marker between pre- and post-hybridisation is used to indicate hybridisation. Therefore, label-free methods also represent a very attractive approach for bioaffinity and interaction detections because of the real-time monitoring of binding [34]. Recently, several groups have reported electrochemical label-free methods for hybridisation detection. For example, Fang et al. [35] developed a label-free electrochemical detection of DNA hybridisation using ferrocene-containing cationic polythiophene and the neutral backbone, peptide nucleic acid, as the probe which was allowed to hybridise with a DNA sequence. Moreover ferrocene-functionalised cationic polythiophene was also used for the label-free electrochemical detection of DNA by Le Floch et al. [36]. Ferrocene-containing cationic polythiophene interacted electrostatically with the negatively charged phosphate groups on the DNA backbone. In this way, oxidation signals obtained in cyclic voltammetry and differential pulse voltammetry of ferrocene in polythiophene were used to indicate hybridisation. However, the use of electroactive species-containing polymers for label-free electrochemical detection of DNA methods suffered from high steric and kinetic barriers to hybridisation arising from constraints in the orientation of the probe DNA sequences within the polymer, and the possibility of oxidative damage to the probe and target oligonucleotides.

Ferrocene is widely used as an electroactive marker for electrochemical DNA detection because of its redox reversibility and its versatile derivatives for various cross-linking reactions [37, 38]. Moreover, ferrocene and most of its derivatives are neutral compounds that remain stable in water and air. As an example, Fan et al. [39] developed an electrochemical DNA sensor by immobilising a DNA stem–loop conjugated with ferrocene on a gold electrode surface. After hybridisation, the surface-confined DNA loop structure induced a large conformational change, which in turn significantly reduced the electron-transfer tunnelling distance between the electrode and the ferrocene label. The resulting change in electron-transfer efficiency was readily measured by cyclic voltammetry.

More recently, the tetravalent metal cation, Zr(IV), has been employed in the detection of nucleic acids [40]. In such work, pectin molecules (a polymer of 300–1,000 α-galacturonic acid units with a variable number of $–COOCH_3$ groups joined with $1\alpha \rightarrow 4$ linkages) were attached to double-stranded DNA (dsDNA) sequences on a chip surface by activation via zirconium–phosphate–carboxylate chemistries. The chips were then incubated in an ammonium silver nitrate solution, from which silver was chemically reduced on the pectin backbone to yield a signal that indicates DNA target hybridisation. Among the cations (e.g. Ca (II), Mn(II)), properties of Zr(IV) ion such as a strong ionic and coordinative interaction between the Zr(IV) ion coordinated to phosphonate and phosphate groups and carboxylate and sulfonate functionalities make it an ideal adhesive reagent in fabricating electrochemical biosensors [41].

In this work, we aim to develop a label-free electrochemical DNA sensor consisting of a carbon nanofiber–chitosan-modified glassy carbon electrode. Then a ssDNA probe was immobilised by covalently coupling the amino group on the

ssDNA probe to amino groups of chitosan in the layer via glutaraldehyde as a linker [42]. The probe was then allowed to hybridise with a DNA target to form a dsDNA. Next, dsDNA sequences on the modified electrode were incubated in a Zr(IV) solution to promote coordinative interaction between Zr(IV) and the dsDNA via phosphate group in the DNA backbone. Zr(IV) ions would then interact with negatively charged carboxyl groups of ferrocenecarboxylic acid used as an electrochemical label in cyclic voltammetric and differential pulse voltammetric detection of hybridisation. In our work, we also employed a two-factorial design to identify the significant operational parameters and their possible interactions for developing the biosensor composition.

Experimental

Reagents

Carbon nanofibres were donated by Dr X. Zhang from World Precision Instruments Inc., Sarasota, USA. Chitosan of medium molecular weight, glutaraldehyde (25% *v*/*v* aqueous solution), ferrocenecarboxylic acid, zirconyl chloride octahydrate, analytical-grade disodium phosphate, potassium hydrogen phosphate and potassium chloride were all purchased from Aldrich (Sydney, Australia). Alumina powder (0.05, 0.3 and 1 μm) was purchased from Leco Corporation, USA.

Oligonucleotides of the following 5′- to 3′-base sequences were purchased from Invitrogen Australia Pty Ltd (Melbourne, Australia):

DNA probe	NH_2-GAG CGC GCT CAG GTG GA
Complementary/target DNA	TCC ACC TGA GCG CGC TC
Three-point mismatched DNA	TCC ATC TGC GCG CAC TC
Non-complementary DNA	GAG CGA GTC TTA ACT AG

Stock solutions of ssDNA were prepared with Tris–EDTA buffer (20 mM Tris–HCl, 1 mM EDTA, pH 8.0). Solutions used in all experiments were prepared with milliQ water obtained from a Millipore-MilliQ system. Phosphate-buffered saline (PBS), adjusted to pH 7.4 by adding 0.1 M NaOH, was employed as a supporting electrolyte.

Cyclic voltammetry and differential pulse voltammetry (scan rate, 50 mV s^{-1}; pulse width, 50 ms, pulse height= 25 mV) were performed using a Powerlab 2120 potentiostat (eDAQ Pty Ltd, Sydney, Australia), which was connected to a personal computer via a 2.0 EChem software (eDAQ Pty Ltd). A three-electrode system, consisting of a platinum wire auxiliary electrode, a Ag|AgCl|KCl (saturated) reference electrode (Bioanalytical Systems Inc., West Lafayette, IN, USA) and a 3-mm-diameter glassy carbon working electrode (Bioanalytical Systems Inc.) was used. Unless stated otherwise, the glassy carbon electrode was modified as described below before use. Prior to voltammetric experiments, all electrolyte solutions were deoxygenated with nitrogen gas for 30 min.

Preparation of chitosan solutions and carboxylic-functionalised carbon nanofibres

Chitosan solution (1% *w*/*v*) was prepared by dissolving chitosan in 1% (*v*/*v*) acetic acid solution. The chitosan solution was filtered to remove any undissolved materials before 0.1 M NaOH was added to adjust the pH of the solution to approximately 5.0. The solution was refrigerated at 4 °C before use.

Carbon nanofibres were functionalised with carboxylic groups as described previously [31]. Briefly, 20 mg of carbon nanofibres was dispersed in 30 mL of 30% (*v*/*v*) HNO_3 and was then refluxed for 24 h at 140 °C. The suspension solution was centrifuged and the carboxylic-functionalised carbon nanofibres were washed with doubly distilled water until the pH reached 7.0. The carbon nanofibres obtained were dried under vacuum at 100 °C.

Preparation of glutaraldehyde|carbon nanofibre|chitosan-modified glassy carbon electrodes

Initially, a 5 mg mL^{-1} carbon nanofibre suspension in chitosan was ultrasonicated for 6 h to obtain a homogeneous solution. A glassy carbon electrode was sequentially polished to a mirror finish using a slurry of 1.0, 0.3 and 0.05 μm alumina powder, rinsed with doubly distilled water, and then sonicated with absolute ethanol and doubly distilled water again to remove any excess absorbents. A 5-μL aliquot of the 5 mg mL^{-1} carbon nanofibre|chitosan solution was applied to the pretreated glassy carbon electrode and dried in air to obtain a carbon nanofibre|chitosan layer-modified electrode. This electrode was then immersed in 3.0% (*v*/*v*) glutaraldehyde for 60 min, followed by rinsing with doubly distilled water to remove any excess glutaraldehyde. Next, the modified electrode was characterised by cyclic voltammetry of the redox markers, 1.0 mM $[Fe(CN)_6]^{3-}$and 1.0 mM $[Fe(CN)_6]^{4-}$, in 0.10 M KCl as a supporting electrolyte at 100 mV s^{-1}.

Immobilisation and hybridisation of DNA on glutaraldehyde|carbon nanofibre|chitosan-modified electrodes

Initially, ssDNA was immobilised on a glutaraldehyde|carbon nanofibre|chitosan-modified electrode by applying a 3-μL

aliquot of a 10 μM DNA probe on the electrode, which was left to dry for 60 min. This electrode was rinsed with 20 mM Tris–EDTA buffer for 5 min to remove any unbound oligonucleotides. Next, the modified electrode was incubated in 10 mM Zr(IV) solution for 30 min and then rinsed with PBS to remove unbound Zr(IV). Differential pulse voltammetry of 1.0 mM ferrocenecarboxylic acid (in pH 7.4 PBS as supporting electrolyte) was conducted at the Zr(IV)|ssDNA|glutaraldehyde|carbon nanofibre-chitosan|glassy carbon electrode between −0.2 V and 0.8 V. The electrode was then rinsed with doubly distilled water before being allowed to hybridise with complementary DNA of specific concentrations (2–10 nM) at 37 °C for 30 min. Following this, the electrode was rinsed with 20 mM Tris–EDTA buffer and doubly distilled water to remove any non-hybridised oligonucleotides. The dsDNA|glutaraldehyde|carbon nanofibre-chitosan|glassy carbon electrode was then incubated in 10 mM Zr(IV) solution for 30 min and washed with PBS to remove any non-specifically bound Zr(IV) to the phosphate groups on the DNA backbone. Differential pulse voltammetry of 1.0 mM ferrocenecarboxylic acid were conducted at the electrode in pH 7.4 PBS as supporting electrolyte between −0.2 V and 0.8 V. In separate experiments, the DNA probe was also allowed to hybridise with the 3-mismatched target, the non-complementary sequence, respectively, using the same procedure. The DNA hybridisation event was assessed by the difference in oxidation peak current (ΔI_p) of ferrocenecarboxylic acid before and after hybridisation. In our precision and stability study, the DNA target was detached in a Tris–EDTA buffer (pH 8.0) at 100 °C for 5 min before the biosensor was re-used.

Statistical analysis

A two-level factorial design [43] was used to identify the principal factors, and their possible interactions, in determining the optimal composition of the glutaraldehyde|carbon nanofibre-chitosan layer on a glassy carbon electrode. Statistical significance of correlation coefficients was tested using Student's *t* test.

Results and discussion

In this work, we have developed a DNA biosensor based on a glassy carbon electrode initially modified by a chitosan layer entrapped with carbon nanofibres. Using glutaraldehye, this composite layer was then carboxylated to attach to the amino group on a DNA probe, which would then hybridise with its complementary DNA target. After coordinating Zr(IV) in the DNA duplex, differential pulse voltammetry of ferrocenecarboxylic acid was conducted at this biosensor to assess hybridisation. In the following sections, the characteristics of each component were systematically studied after it was assembled on the biosensor surface, including an optimisation of the composition of the anchoring glutaraldehyde|carbon nanofibre|chitosan layer using a two-factorial design.

Electrochemical characterisation of carbon nanofibre|chitosan composite layer on glassy carbon electrodes

According to Olenic et al. [44], it is difficult to dissolve carbon nanofibres in water and acid solutions owing to hydrophobic interactions and van der Wall's attractive forces between the aggregated nanofibres. However, carbon nanofibres became soluble after being functionalised with –COOH and –OH groups using concentrated nitric acid. As chitosan is a cationic biopolymer, it is suitably used as a medium for carbon nanofibres containing anionic $–COO^-$ to form a homogeneous dispersion. Similar scanning electron micrographs (data not shown) to those demonstrated previously [26] showed that the carbon nanofibre|chitosan layer formed a smooth, homogeneous and porous membrane on the glassy carbon electrode. In this work, the presence of a carbon nanofibre|chitosan layer on a glassy carbon electrode was also evaluated by the cyclic voltammetry of the commonly used system of 1.0 mM $[Fe(CN)_6]^{3-}$ and 1.0 mM $[Fe(CN)_6]^{4-}$ in 0.10 M KCl as a supporting electrolyte at 100 mV s^{-1}. The results obtained are shown in Fig. 1. Initially, cyclic voltammogram of the $[Fe(CN)_6]^{3-}$/$[Fe(CN)_6]^{4-}$ redox couple at a bare glassy carbon electrode, depicted in trace a, shows an oxidation peak at approximately 0.29 V and a reduction peak at 0.18 V. When cyclic voltammetry was repeated at a chitosan-coated glassy carbon electrode, the result (trace b) shows a pair of redox peaks with essentially unchanged peak potentials but a 118% increase in current compared to that obtained at the bare glassy carbon electrode. This is attributable to electrostatic attraction of the negatively charged $[Fe(CN)_6]^{3-}$/$[Fe(CN)_6]^{4-}$ towards the positively charged amine-bearing chitosan layer. Similarly, the cyclic voltammogram obtained at a carbon nanofibre|chitosan-modified glassy carbon electrode, displayed in trace c, shows a pair of redox peaks at similar potentials but a 126% increase in current, relative to that obtained in trace b, owing to a further increase in surface area by the carbon fibres entrapped within the chitosan layer.

Optimisation of the glutaraldehyde|chitosan|carbon nanofibre layer on a glassy carbon electrode

To immobilise the DNA probe on the electrode surface, we have used the homo-bifunctional crosslinker, glutaraldehye, to covalently bond to the primary amine groups of chitosan at one end, and to an amino group at the 5′-terminal of a ssDNA probe at the other end. Notably, the three factors, concentration of chitosan (denoted as X_1), concentration of carbon nanofibres (X_2), and the incubation time in

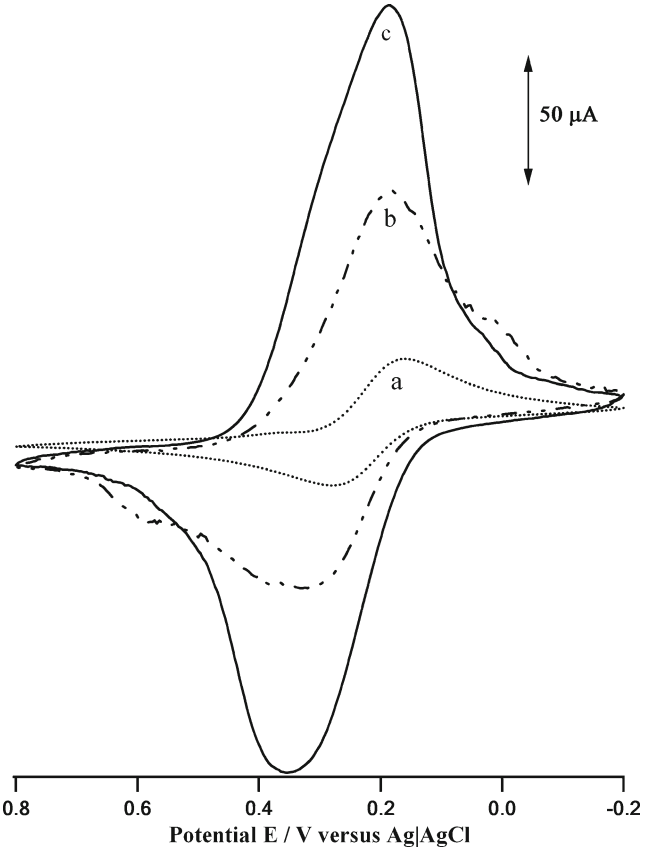

Fig. 1 Cyclic voltammograms of 1.0 mM $[Fe(CN)_6]^{3-}$ and 1.0 mM $[Fe(CN)_6]^{4-}$ in 0.10 M KCl at (*a*) a bare glassy carbon electrode, (*b*) a chitosan|glassy carbon electrode, (*c*) a carbon nanofibre|chitosan|glassy carbon electrode; scan rate=100 mV s^{-1}

glutaraldehye (X_3), will contribute to the optimum composition of the anchoring layer for the DNA probe. In this work, we have employed a 2^3-factorial design to identify the significant factors and their possible interactions. The experimental factors and their levels employed in a 2^3-factorial design are shown in Table 1. The low and high levels were designated for each factor to construct the different computation of factors and their interactions in a 2^3-factorial design as shown in Table 2. Two replicated cyclic voltammetric scans of 1.0 mM $[Fe(CN)_6]^{3-}$and 1.0 mM $[Fe(CN)_6]^{4-}$in 0.10 M KCl as a supporting electrolyte at 100 mV s^{-1} were conducted at each condition by following a randomised order of experiment (refer to column 9 in Table 2). In addition, Table 2 shows the different computations involving both factors and their interactions (X_1X_2, X_1X_3, X_2X_3 and $X_1X_2X_3$) in a 2^3 factorial design. The t_E in Table 2 represents a signal-to-noise ratio evaluated by Eq. 1,

$$t_E = \frac{\text{Effect}}{2s_p/n_F} \quad (1)$$

In this equation, Effect represents the average between the high (+) and the low (−) values of each experimental parameter and n_F is the number of experimentation for two replications (n_F=16), whereas s_p represents the pooled standard deviation determined by Eq. 2,

$$s_p = \sum_{i=1}^{m} \text{variance}_i \quad (2)$$

Here, m is the number of experimental conditions (m=8). In Table 2, t* represents the tabulated two-tailed t value (2.306) for 8 degrees of freedom at the 95% confidence level. If the value of t_E is larger than t*, the effect of specific factor or interaction between factors is considered significant. Accordingly, in Table 2, X_1, X_2, and the interactions X_1X_2, X_1X_3 are statistically significant in this work. These results are expected. In our work, X_1, X_2 and their interaction (X_1X_2) directly affect the quantity of the respective components of the structure on the sensor, and hence the magnitude of the detection signal. Similarly, amide is formed between the carboxylic acid group of glutaraldehyde and the amino group of chitosan, which accounts for the significance of X_1X_3. However, no reaction is expected between glutaraldehyde and carbon nanofibres, thus X_2X_3 was not found to be significant. Further, X_3 alone does not affect the detection signal. The optimum conditions for factor X_1, X_2 and the interaction X_1X_2, X_1X_3 were then further determined in detecting DNA hybridisation, as shown by the results in Tables 3 and 4, respectively. Here, we obtained X_1=0.5% *w/v*, X_2=5.0 mg mL^{-1} and X_3=60 min of incubation time in glutaraldehyde as the optimal values for all three parameters.

Electrochemical characteristics of DNA probe on glutaraldehyde|carbon nanofibre|chitosan-modified glassy carbon electrodes

In the next construction step, a ssDNA was conjugated to a glutaraldehyde|carbon nanofibre|chitosan-modified electrode, which was then incubated in a solution of a complementary DNA target for 30 min. Similar to Fig. 1, the redox pair, $[Fe(CN)_6]^{3-}/[Fe(CN)_6]^{4-}$, was used to study the

Table 1 Experimental factors and levels assigned in a 2^3-factorial design

Factor	Definition	Label	Low level (−)	High level (+)
1	Concentration of chitosan/% *w/v*	X_1	0.1	1
2	Concentration of carbon nanofibres/mg/mL	X_2	1.0	5
3	Incubation time in glutaraldehyde/min	X_3	10	120

Table 2 The significant computation of effects and interaction for a 2^3 factorial design

Conditions	X_1	X_2	X_3	X_1X_2	X_1X_3	X_2X_3	$X_1X_2X_3$	Run order	I_{oxd}	Average I_{oxd}	Variance
1	−	−	−	+	+	+	−	1, 13	17,15	16	2
2	+	−	−	−	−	+	+	6, 15	28,41	34.5	84.5
3	−	+	−	−	+	−	+	4, 12	60,58	59	2
4	+	+	−	+	−	−	−	8, 9	55,26	40.5	420.5
5	−	−	+	+	−	−	+	5, 14	16,25	20.5	40.5
6	+	−	+	−	+	−	−	3, 11	57,51	54	18
7	−	+	+	−	−	+	−	7, 10	40,33	36.5	24.5
8	+	+	+	+	+	+	+	2, 16	42,58	50	128
Sum product[a]	46	62	12	−56	48	−38	16				
Effect	11.5	15.5	3	−14	12	−9.5	4				
t_E	2.43	3.27	0.633	−2.95	2.53	−2.00	0.844		t^a (8 degrees of freedom) =2.306		

[a] Sum of average I_{oxd} taking into consideration the signs tabulated in the particular column

electrochemical characteristics of the DNA immobilised on a glutaraldehye|carbon nanofibre|chitosan-modified glassy carbon electrode. The cyclic voltammograms obtained are depicted in Fig. 2a. Initially, the cyclic voltammogram of $[Fe(CN)_6]^{3-}/[Fe(CN)_6]^{4-}$ in trace a shows an oxidation peak and a reduction peak at approximately 0.29 and 0.16 V, respectively, at a glutaraldehyde-treated carbon nanofibre| chitosan-modified glassy carbon electrode. After attaching a ssDNA probe on the electrode (trace b), the oxidation peak current decreased by 32.5%, which can be attributed to the repulsion of the negatively charged $[Fe(CN)_6]^{3-}/[Fe(CN)_6]^{4-}$ by the negatively charged phosphate groups in the backbone of the ssDNA probe away from the electrode. The cyclic voltammogram of $[Fe(CN)_6]^{3-}/[Fe(CN)_6]^{4-}$obtained after a DNA duplex was formed on the modified electrode is shown in trace c. In this case, the negatively charged phosphate groups present in the DNA duplex further resisted the approach of $[Fe(CN)_6]^{3-}/[Fe(CN)_6]^{4-}$to the electrode, resulting in a 31.2% decrease in the peak currents.

Interactions between DNA duplex and Zr(IV)

Zr(IV) is an inorganic ion with low systemic toxicity. It has affinity for groups containing oxygen and it is a suitable material for immobilisation of biomolecules with oxygen group [45]. For this reason, Zr(IV) ion was used as a linkage between the phosphate groups of peptide and an oxygen-containing electroactive marker. Accordingly, ferrocenecarboxylic acid, instead of $[Fe(CN)_6]^{3-}/[Fe(CN)_6]^{4-}$, was used as the marker in all subsequent experiments. Figure 2b shows the cyclic voltammograms of 1.0 mM ferrocenecarboxylic acid in pH 7.4 PBS obtained at a bare glassy carbon electrode (trace a) and glutaraldehyde|carbon nanofibre|chitosan-modified glassy carbon electrode (trace b). The oxidation peak current has increased by 241% at the modified glassy carbon electrode, relative to that at a bare electrode, owing to increased charge transfer with increased electrode surface area arising from the incorporated carbon nanofibres. A ssDNA probe was next attached to the electrode, which was then allowed to hybridise with its complementary DNA target. The corresponding cyclic voltammogram acquired is shown in trace c. The oxidation peak current is approximately 85% less than that shown in trace b. This decrease was most likely resulted from the repulsion of the negatively charged ferrocencarboxylic acid by the negatively charged phosphate groups of the DNA sequences on the electrode. Finally, the dsDNA|glutaraldehyde|carbon nanofibre-chitosan|glassy

Table 3 Optimisation of the concentration of chitosan (X_1) and carbon nanofibres (X_2) immobilised on a glassy carbon electrode based on the reduction peak current (in μA) of 1.0 mM $[Fe(CN)_6]^{3-}$ in 0.10 M KCl; scan rate 100 mV s^{-1}

X_2/mg mL^{-1}	X_1/% *w*/*v*		
	0.1	0.5	1.0
1	29.3, 31.6	36.2, 34.0	39.1, 43.7
3	60.7, 63.6	84.5, 80.7	61.7, 65.0
5	80.4, 84.0	145.4, 140.3	119.9, 121.6

Table 4 Optimisation of the concentration of chitosan (X_1) immobilised on a glassy carbon electrode and incubation time of the electrode in glutaraldehyde (X_3) based on the reduction peak current (in μA) of 1.0 mM $[Fe(CN)_6]^{3-}$ in 0.10 M KCl; scan rate=100 mV s^{-1}. Concentration of carbon nanofibres used=5 mg mL^{-1}

X_3/min	X_1/% *w*/*v*		
	0.1	0.5	1.0
1	75.2, 77.0	133.3, 129.7	123.0, 131.5
3	85.7, 88.6	141.5, 137.8	132.6, 128.0
5	81.4, 84.3	130.4, 136.3	127.9, 125.2

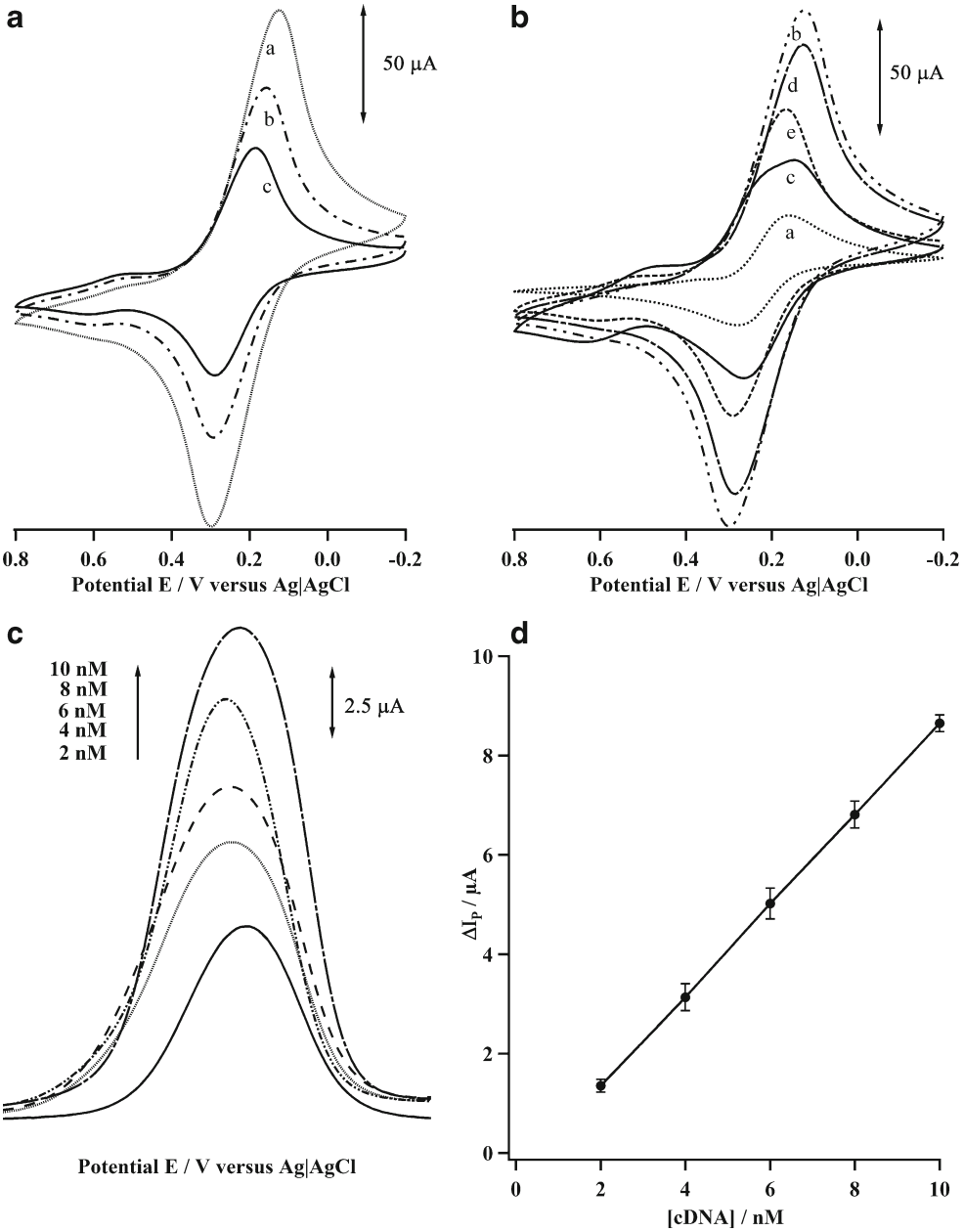

Fig. 2 **a** Cyclic voltammograms of 1.0 mM $[Fe(CN)_6]^{3-}$/and 1.0 mM $[Fe(CN)_6]^{4-}$ in 0.10 M KCl at (*a*) a glutaraldehyde|carbon nanofibre|chitosan|glassy carbon electrode, (*b*) a ssDNA|glutaraldehyde|carbon nanofibre|chitosan|glassy carbon electrode, (*c*) a dsDNA| glutaraldehyde|carbon nanofibre|chitosan|glassy carbon electrode; scan rate= 100 mV s^{-1}. **b** Cyclic voltammograms of 1.0 mM ferrocenecarboxylic acid in PBS (pH 7.4) at (*a*) a bare glassy carbon electrode, (*b*) a glutaraldehyde|carbon nanofibre|chitosan|glassy carbon electrode, (*c*) a dsDNA|glutaraldehyde|carbon nanofibre|chitosan|glassy carbon electrode, (*d*) a Zr(IV)|dsDNA|glutaraldehyde| carbon nanofibre|chitosan|glassy carbon electrode, (*e*) a Zr(IV)|ssDNA|glutaraldehyde| carbon nanofibre|chitosan|glassy carbon electrode; scan rate=100 mV s^{-1}. **c** Differential pulse voltammograms of 1.0 mM ferrocenecarboxylic acid at a Zr(IV)|dsDNA|glutaraldehyde|carbon nanofibre|chitosan|glassy carbon electrode in the indicated complementary DNA target concentration in PBS (pH 7.4), after subtracting away the differential pulse voltammogram at the corresponding Zr(IV)|ssDNA|glutaraldehyde|carbon nanofibre|chitosan|glassy carbon electrode; scan rate=50 mV s^{-1}. **d** A calibration plot constructed based on peak current shown in Fig. 2c

carbon electrode was incubated in 10 mM Zr(IV) solution for 30 min before being used to obtain the cyclic voltammogram of ferrocenecarboxylic acid depicted in trace d. In this case, upon the incorporation of a high loading of strong positive Zr (IV) ions between the dsDNA sequences with additional phosphate groups, more ferrocecarboxylic acid was attracted to the electrode surface for oxidation, resulting in an enhanced peak current in trace d compared to trace c. For comparison, we have also conducted cyclic voltammetry of ferrocenecarboxylic acid at a Zr(IV)-loaded ssDNA|glutaraldehyde|carbon nanofibre-chitosan|glassy carbon electrode and the result is shown in trace e. Note that the oxidation peak current in trace e is almost 36% higher than that shown in trace c because of the electrostatic attraction of ferrocenecarboxylic acid by the Zr(IV)-loaded layer towards the electrode for oxidation. In this work, the change in current between trace d and trace e was used to indicate hybridisation between the DNA probe and its complementary DNA target.

Analytical applications

Differential pulse voltammetry was used here as a sensitive detection technique for the oxidation of 1.0 mM ferrocenecarboxylic acid at a Zr(IV)|dsDNA|glutaraldehyde|carbon nanofibre-chitosan|glassy carbon electrode, under the optimum conditions of 5.0 mg mL^{-1} carbon nanofibres in 0.5%

Table 5 Comparison of analytical performance of DNA biosensors

	Linear range	Limit of detection (pM)
Floch et al., 2005	1 nM–1 μM	500
Liao et al., 2006	100 pM–100 nM	100
Li et al., 2009	0.045 nM–1.57 nM	326
Cai et al., 2010	1 pM–1000 pM	0.1
Our work	0.5 nM–40 nM	88

(*w*/*v*) chitosan in 1.0% (*v*/*v*) acetic acid solution, after the electrode was incubated in complementary DNA target solutions of concentration between 2 nM and 10 nM. Figure 2c shows the differential pulse voltammograms obtained in these DNA target solutions after subtracting away the differential pulse voltammogram obtained at the corresponding Zr(IV)|ssDNA|glutaraldehyde|carbon nanofibre|chitosan|glassy carbon electrode. A calibration plot based on the peak current measured in Fig. 2c is shown in Fig. 2d. The difference in peak current (ΔI_p) of ferrocenecarboxylic acid before and after hybridisation was observed to increase linearly with the DNA target concentration with a correlation coefficient of 0.9999 (N=5), which was found to be statistically significant at the 95% confidence level. This relationship can be represented by the expression,

$$\Delta I_p/\mu A = \left(0.91 \pm 0.25/\mu A\ nM^{-1}\right)[\text{DNAtarget}] - (0.049 \pm 0.042\mu A)$$

where the errors represent the 95%confidence intervals. Based on a signal-to-noise ratio of 3, a detection limit of 88 pM was estimated. In addition, a dynamic range of 0.5–40 nM was determined. For comparison, the detection limits achieved at several recently developed electrochemical DNA biosensors are tabulated in Table 5. Notably, our detection limit and dynamic range compare favourably to many of these biosensors. In our work, Zr(IV) electrostatically attracted ferrocenecarboxylic acid in solution towards the DNA biosensor for oxidation. In addition, the DNA probe was aligned freely on the biosensor for hybridisation with its target. Minimised steric hindrance, compared to the ferrocene-functionalised cationic polythiophene-coated label-free DNA biosensor [36], would have contributed to a lower detection limit at our biosensor. Similarly, enhancement of surface area by carbon nanofibres has allowed a large loading of all biological components in our biosensor, leading to a lower detection limit compared to that involving diazotisation-coupling on self-assembled 4-aminothiophenol for DNA probe immobilisation [46]. Although a similar detection limit was reported at a DNA biosensor involving a ferrocenyl peptide conjugated probe [33], an additional step involving the use of the organic reagent dichloromethane was required. Cai et al. [47] developed a stable magnetic bead-based DNA sensor monitored by comparing chemiluminescence changes in the absence and presence of DNA targets. Unfortunately, such stabilisation of the duplex structure required a stringent temperature control.

Selectivity of electrochemical DNA sensor

The selectivity of DNA sensor was investigated based on the oxidation current of 1.0 mM ferrocenecarboxylic acid in pH 7.4 PBS at the ssDNA|carbon nanofibre|chitosan-modified electrode after being incubated in 30 nM complementary, non-complementary and three-base mismatched oligonucleotides, respectively. The results, shown in Fig. 3a, indicate an average ΔI_p of 32.0, 11.5 and 2.10 μA, at the complementary, 3-mismatch and non-complementary oligonucleotides, respectively. Notably, when the complementary sequence was used as the target for DNA probe, the peak current was 64% and 93% higher than the 3-mismatch and non-complementary oligonucleotides, respectively. This indicates that the fabricated

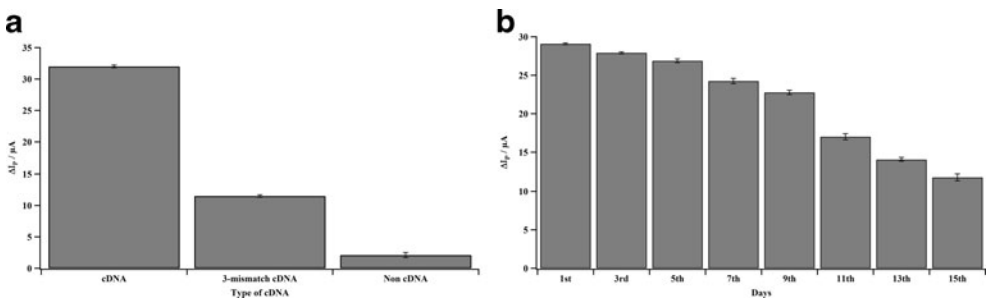

Fig. 3 Histograms showing the ΔI_p of 1.0 mM ferrocenecarboxylic acid in PBS (pH 7.4) after the electrochemical DNA sensor was incubated in **A** a complementary DNA (cDNA), a three-point mismatched DNA and a non-complementary DNA, **B** a complementary DNA over a 15-day period

DNA sensor was selective for detecting the different sequences of target oligonucleotides.

Precision and stability study

The precision and stability of the fabricated DNA sensor were studied. In the precision study, the reproducibility (intra-assay) and repeatability (inter-assay) of the DNA sensor were tested at three different concentrations of complementary oligonucleotides at 5, 15 and 30 nM. Intra-assays of these samples were performed in four duplicates with the same DNA sensor and inter-assays with different DNA sensors using the same manufactured batch. For intra-assays, the relative standard deviation (RSD; N=4) varied from 1.9% to 4.7%, while that for inter-assay varied from 2.3% to 3.0%. The small RSD showed that our DNA sensor fabrication procedure is reliable. The stability of the DNA sensor was investigated by measuring its cyclic voltammetric response of 1.0 mM ferrocenecarboxylic acid at the electrode in pH 7.4 PBS as supporting electrolyte between −0.2 and 0.8 V. The results obtained using 30 nM complementary oligonucleotide are shown in Fig. 3b. The cyclic voltammetric responses of DNA sensors were compared to those obtained on the first day. An average response decrease of 2.1% was observed after 2 days, 15% after 1 week and 50% after 2 weeks. The obtained results were most likely caused by damage of DNA sensor in the de-hybridisation step used to regenerate a ssDNA|glutaraldehyde|carbon nanofibre|chitosan| glassy carbon electrode for repeated use, as sensors without being treated by the de-hybridisation step showed negligible change in their response after 2 weeks.

Conclusion

An electrochemical DNA biosensor for hybridisation detection based on a ssDNA|glutaraldehye|carbon nanofibre|chitosan-modified glassy carbon electrode has been developed with sensitivity and selectivity. In this design, carbon nanofibres were used as nanomaterial to increase the electrode surface area to support a high loading of ssDNA probe and hence lower the detection limit of DNA target. Based on a 2^3-factorial design, we have constructed an anchoring layer of optimal composition of 5.0 mg mL^{-1} carbon nanofibre in 0.5% (w/v) chitosan on a glassy carbon electrode that was incubated in glutaraldehyde for 60 min. A 17-base pair DNA probe was attached to the modified electrode, followed by its complementary DNA target. Positive Zr(IV) ions were coordinated between negative phosphate groups of DNA sequences before and after hybridisation. The change in oxidation peak current of ferrocenecarboxylic acid at the biosensor surface was used to indicate hybridisation in the label-free detection method developed in this work. Accordingly, a dynamic range between 0.50 and 40 nM and a detection limit of 88 pM were obtained. In addition, the selectivity of the DNA biosensor was indicated by insignificant current change when non-complementary DNA targets were used in the hybridisation experiments.

References

1. Erdem A, Ozsoz M (2001) Interaction of the anticancer drug epirubicin with DNA. Anal Chim Acta 437(1):107–114
2. Evtugyn G, Goldfarb O, Budnikov H, Ivanov A, Vinter V (2005) Amperometric DNA-peroxidase sensor for the detection of pharmaceutical preparations. Sensors 5(6):364–376
3. Liao JC, Mastali M, Gau V, Suchard MA, Moller AK, Bruckner DA, Babbitt JT, Li Y, Gornbein J, Landaw EM, McCabe ERB, Churchill BM, Haake DA (2006) Use of electrochemical DNA biosensors for rapid molecular identification of uropathogens in clinical urine specimens. J Clin Microbiol 44(2):561–570
4. Mandong G, Yanqing L, Hongxia G, Xiaoqin W, Lifang F (2007) Electrochemical detection of short sequences related to the hepatitis B virus using MB on chitosan-modified CPE. Bioelectrochemistry 70(2):245–249
5. Chang Z, Chen M, Fan H, Zhao K, Zhuang S, He P, Fang Y (2008) Multilayer membranes via layer-by-layer deposition of PDDA and DNA with Au nanoparticles as tags for DNA biosensing. Electrochim Acta 53(6):2939–2945
6. Divne A-M, Allen M (2005) A DNA microarray system for forensic SNP analysis. Forensic Sci Int 154(2–3):111–121
7. Zhao X, Tapec-Dytioco R, Tan W (2003) Ultrasensitive DNA detection using highly fluorescent bioconjugated nanoparticles. J Am Chem Soc 125(38):11474–11475
8. Miao W, Bard AJ (2004) Electrogenerated chemiluminescence. 77. DNA hybridisation detection at high amplification with [Ru $(bpy)_3]^{2+}$-containing microspheres. Anal Chem 76(18):5379–5386
9. Okahata Y, Kawase M, Niikura K, Ohtake F, Furusawa H, Ebara Y (1998) Kinetic measurements of DNA hybridisation on an oligonucleotide-immobilized 27-MHz quartz crystal microbalance. Anal Chem 70(7):1288–1296
10. Sun HB, Yokota H (2000) MutS-mediated detection of DNA mismatches using atomic force microscopy. Anal Chem 72 (14):3138–3141
11. Guedon P, Livache T, Martin F, Lesbre F, Roget A, Bidan G, Levy Y (2000) Characterisation and optimisation of a real-time, parallel, label-free, polypyrrole-based DNA sensor by surface plasmon resonance imaging. Anal Chem 72(24):6003–6009
12. Liu T, Ja T, Jiang L (2004) The enhancement effect of gold nanoparticles as a surface modifier on DNA sensor sensitivity. Biochem Biophys Res Commun 313(1):3–7
13. Lucarelli F, Tombelli S, Minunni M, Marrazza G, Mascini M (2008) Electrochemical and piezoelectric DNA biosensors for hybridisation detection. Anal Chim Acta 609(2):139–159
14. Zhu N, Chang Z, He P, Fang Y (2005) Electrochemical DNA biosensors based on platinum nanoparticles combined carbon nanotubes. Anal Chim Acta 545(1):21–26
15. Dharuman V, Hahn JH (2008) Label free electrochemical DNA hybridisation discrimination effects at the binary and ternary mixed monolayers of single stranded DNA/diluent/s in presence of cationic intercalators. Biosens Bioelectron 23(8):1250–1258
16. Carrara S, Gurkaynak F, Guiducci C, Stagni C, Benini L, Leblebici Y, Samorì B, De Micheli G (2007) Interface layering phenomena in capacitance detection of DNA with biochips. Sens Trans J 76:969–977

17. Park J-Y, Park S-M (2009) DNA hybridisation sensors based on electrochemical impedance spectroscopy as a detection tool. Sensors 9(12):9513–9532
18. Loaiza ÓA, Campuzano S, Prada AG-Vd, Pedrero M, Pingarrón JM (2008) Amperometric DNA quantification based on the use of peroxidase-mercaptopropionic acid-modified gold electrodes. Sensors Actuators B Chem 132(1):250–257
19. Olofsson L, Rindzevicius T, Pfeiffer I, Käll M, Höök F (2003) Surface-based gold-nanoparticle sensor for specific and quantitative DNA hybridisation detection. Langmuir 19(24):10414–10419
20. Li G, Li X, Wan J, Zhang S (2009) Dendrimers-based DNA biosensors for highly sensitive electrochemical detection of DNA hybridisation using reporter probe DNA modified with Au nanoparticles. Biosens Bioelectron 24(11):3281–3287
21. Gao M, Qi H, Gao Q, Zhang C (2008) Electrochemical detection of DNA hybridisation based on the probe labeled with carbon-nanotubes loaded with silver nanoparticles. Electroanalysis 20(2):123–130
22. Wang J, Liu G, Rasul Jan M, Zhu Q (2003) Electrochemical detection of DNA hybridisation based on carbon-nanotubes loaded with CdS tags. Electrochem Commun 5(12):1000–1004
23. Qiu J-D, Zhou W-M, Guo J, Wang R, Liang R-P (2009) Amperometric sensor based on ferrocene-modified multiwalled carbon nanotube nanocomposites as electron mediator for the determination of glucose. Anal Biochem 385(2):264–269
24. Wang J, Kawde A-N, Jan MR (2004) Carbon-nanotube-modified electrodes for amplified enzyme-based electrical detection of DNA hybridisation. Biosens Bioelectron 20(5):995–1000
25. Gu CP, Huang JR, Wang JH, Wang CJ, Li MQ, Liu JH (2007) Enhanced electrochemical detection of DNA hybridisation based on Au/MWCNTs nanocomposites. Anal Lett 40(17):3159–3169
26. Wu L, Zhang X, Ju H (2007) Highly sensitive flow injection detection of hydrogen peroxide with high throughput using a carbon nanofiber-modified electrode. Analyst 132(5):406–408
27. Wang F, Li D, Li G, Liu X, Dong S (2008) Electrodissolution of inorganic ions/DNA multilayer film for tunable DNA release. Biomacromolecules 9(10):2645–2652
28. Vamvakaki V, Fouskaki M, Chaniotakis N (2007) Electrochemical biosensing systems based on carbon nanotubes and carbon nanofibers. Anal Lett 40(12):2271–2287
29. Wang J, Lin Y (2008) Functionalised carbon nanotubes and nanofibers for biosensing applications. TrAC Trends Anal Chem 27 (7):619–626
30. Wu L, McIntosh M, Zhang X, Ju H (2007) Amperometric sensor for ethanol based on one-step electropolymerisation of thionine–carbon nanofiber nanocomposite containing alcohol oxidase. Talanta 74(3):387–392
31. Hao C, Ding L, Zhang X, Ju H (2007) Biocompatible conductive architecture of carbon nanofiber-doped chitosan prepared with controllable electrodeposition for cytosensing. Anal Chem 79 (12):4442–4447
32. Levine PM, Gong P, Levicky R, Shepard KL (2009) Real-time, multiplexed electrochemical DNA detection using an active complementary metal-oxide-semiconductor biosensor array with integrated sensor electronics. Biosens Bioelectron 24(7):1995–2001
33. Liao LB, Xiao XM (2006) Electronic detection of DNA utilising ferrocenyl peptide conjugates probe. Sensor Actuators B Chem 115(1):465–472
34. Vagin MY, Trashin SA, Karyakin AA, Mascini M (2008) Label-free detection of DNA hybridisation at a liquid|liquid interface. Anal Chem 80(4):1336–1340
35. Fang B, Jiao S, Li M, Qu Y, Jiang X (2008) Label-free electrochemical detection of DNA using ferrocene-containing cationic polythiophene and PNA probes on nanogold modified electrodes. Biosens Bioelectron 23(7):1175–1179
36. Le Floch F, Ho HA, Harding-Lepage P, Bédard M, Neagu-Plesu R, Leclerc M (2005) Ferrocene-functionalised cationic polythiophene for the label-free electrochemical detection of DNA. Adv Mater 17 (10):1251–1254
37. Anne A, Bouchardon A, Moiroux J (2003) 3′-Ferrocene-labeled oligonucleotide chains end-tethered to gold electrode surfaces: novel model systems for exploring flexibility of short DNA using cyclic voltammetry. J Am Chem Soc 125(5):1112–1113
38. Okochi M, Ohta H, Tanaka T, Matsunaga T (2005) Electrochemical probe for on-chip type flow immunoassay: immunoglobulin G labeled with ferrocenecarboaldehyde. Biotechnol Bioeng 90 (1):14–19
39. Fan C, Plaxco KW, Heeger AJ (2003) Electrochemical interrogation of conformational changes as a reagentless method for the sequence-specific detection of DNA. PNAS 100(16):9134–9137
40. Wang J, Wang F, Xu Z, Wang Y, Dong S (2007) Surface plasmon resonance and electrochemistry characterisation of layer-by-layer self-assembled DNA and Zr^{4+} thin films, and their interaction with cytochrome c. Talanta 74(1):104–109
41. Mazur M, Krysiński P, Michota-Kamińska A, Bukowska J, Rogalski J, Blanchard GJ (2007) Immobilisation of laccase on gold, silver and indium tin oxide by zirconium–phosphonate–carboxylate (ZPC) coordination chemistry. Bioelectrochemistry 71 (1):15–22
42. Ge C, Miao W, Ji M, Gu N (2005) Glutaraldehyde-modified electrode for nonlabeling voltammetric detection of *p16^{INK4A}* gene. Anal Bioanal Chem 383(4):651–659
43. Erjavec JLaJ (2001) Modern statistics for engineering and quality improvement. Pacific Grove, CA: Duxbury Chapter 8
44. Olenic L, Mihailescu G, Pruneanu S, Lupu D, Biris A, Margineanu P, Garabagiu S (2009) Investigation of carbon nanofibers as support for bioactive substances. J Mater Sci Mater Med 20(1):177–183
45. Wang Z, Yang Y, Leng K, Li J, Zheng F, Shen G, Yu R (2008) A sequence–selective electrochemical DNA biosensor based on HRP–labeled probe for colorectal cancer DNA detection. Anal Lett 41(1):24–35
46. Li F, Chen W, Dong P, Zhang S (2009) A simple strategy of probe DNA immobilisation by diazotisation-coupling on self-assembled 4-aminothiophenol for DNA electrochemical biosensor. Biosens Bioelectron 24(7):2160–2164
47. Cai S, Lau C, Lu J (2010) Sequence-specific detection of short-length DNA via template-dependent surface-hybridisation events. Anal Chem 82(17):7178–7184